

Synthesis and photocatalytic properties of dense and porous TiO₂ - anatase thin films prepared by sol-gel

N. Arconada, Y. Castro, A. Durán

Instituto de Cerámica y Vidrio (CSIC), Campus de Cantoblanco, 28049 Madrid, Spain

S. Suárez, R. Portela, J. M. Coronado, B. Sánchez

CIEMAT-PSA, Avda Complutense 22, 28040 Madrid, Spain

Corresponding authors: e-mail: castro@icv.csic.es

Abstract

Porous TiO₂-anatase films were prepared by sol-gel route showing higher photocatalytic activity in degradation of trichloroethylene (TCE) in air compared to dense titania films. Thus, titania sols were synthesized with and without a pore generating agent, polyethylene glycol (PEG), to evaluate the effect of porosity in the photocatalytic activity of the coatings. The films were deposited by dipping and sintered at different temperature and time. The characterisation was performed by profilometry, Fourier Transform Infrared Spectroscopy (FTIR), Grazing X-ray Diffraction (GXRD) and Field Emission Scan Electron Microscopy (FE-SEM), observing that anatase phase is obtained at temperatures as low as 350 °C. The maximum specific surface area ($S_s = 43 \text{ m}^2/\text{gr}$) was obtained for coatings prepared from TiO₂ sol with PEG and sintered at 400 °C. Porous TiO₂ – anatase films present trichloroethylene (TCE) conversion around twenty percent higher than that of dense films. Porous volume, surface area and thickness of the coating play a key role in the photocatalytic activity. On the other side, variation in particle size seems not to be a critical parameter in the studied range.

Keywords: sol-gel TiO₂ coatings, template (PEG), photocatalysis, trichloroethylene.

1. INTRODUCTION

Volatile Organic Compounds (VOC's) are recognized among the dangerous pollutant compounds. Besides of being carcinogen agents and contribute to ozone production in the troposphere [1, 2]; the major problem arises from their high resistance to physical, chemical or biological treatments. The paint and adhesive industry, as well as combustion processes are among the most important anthropogenic sources of VOC's emissions into the atmosphere [3].

Photocatalysis is an efficient, attractive and clean technology for pollutant abatement either in aqueous media or in gas phase [4, 5]. TiO_2 is the archetypical photocatalytic material since it is endowed with an inherent photocatalytic activity [6, 7]. Besides, it is inexpensive, very stable and available in large amounts. Specially for air treatment the usage of TiO_2 particles is not feasible due to the high costs of the concomitant filtration facilities needed to recover the catalyst and the risk to release TiO_2 particles into the atmosphere. Therefore, processes focused on the development of supported catalysts with high photocatalytic performance are receiving great attention in the last years either in air [8, 9] or water treatment [10- 12].

Different methods have been used to prepare TiO_2 films: reactive method [13], chemical vapour deposition, sputtering, pulsed laser deposition (PLD) [14] or hydrothermal method [15]. But sol-gel process is considered as one of the most promising alternatives because it presents a number of advantages such as low sintering temperature, versatility of processing and homogeneity at molecular level. This method allows obtaining TiO_2 -anatase at low temperature.—This phase has been extensively investigated because its high activity in photocatalytic applications [16, 17].

TiO_2 powders and gels with porous structure and high photocatalytic performance have been reported [18, 19]. However, the preparation of porous TiO_2 films with high specific surface is attracting more and more attention [20-22]. Photocatalytic processes are chemical reactions on the surface. Thus, the increase of surface area should improve the efficiency of the process because it implicates larger contact surfaces exposed to the pollutants [23, 24].

Porous inorganic TiO_2 -anatase films can be obtained using templating membranes [25] or conventional alkoxide sol-gel route with the addition of surfactants [26] The templates permit to retain the initial polymer morphology up to final porous structure. Polyethylene-glycol is especially suitable for modifying the porous structure of coatings [27, 28] due to its complete decomposition at relatively low temperature

[29,30]. However, the control of synthesis and deposition processes is crucial for obtaining thick, crack-free and homogeneous coatings with good.

Crystalline phase, specific surface area, surface OH groups, morphology and aggregation of particles are some of the parameters playing a decisive role in the photocatalytic efficiency of titania [31, 32]. However, diverse results can be found in literature. While some authors highlight the high surface area as determining factor to increase efficiency [33, 34, ³⁵] others point out the influence of crystallinity and particle size [36].

The aim of this work was to investigate the photocatalytic activity of porous TiO₂ - anatase coatings as a function of surface area, porosity, crystallinity and particle size using trichloroethylene (TCE) as VOC molecule. This compound has been widely used as a model pollutant in semiconductor photocatalysis because it can be easily photodegraded.

Porous coatings were prepared using a simple and easy to scale-up alkoxide route by adding polyethylene glycol (PEG) as pore generating agent. Dense nanocrystalline TiO₂-anatase thin films used as reference were also synthesized. The synthesis and heat treatment conditions were optimised for obtaining coatings with high crystallinity and surface area. An innovative method to determine surface area of coatings is also described.

2. EXPERIMENTAL

2.1 Synthesis and characterisation of sols

Synthesis of sols. Two titania sols (sol A and sol B) were prepared using titanium isopropoxide (TISP) as precursor via acid catalysis with the following route. First, TISP was chemically modified by adding acetyl-acetone (AcAc) to control the hydrolysis and condensation reactions. This solution was maintained for 1 hour under stirring up to obtain the complex chelate. Ethanol mixed with acidified water (0.1 N HCl) was added drop by drop to this solution to start hydrolysis and condensation reactions. The final molar ratio of sol-A was 1 TISP: 1 AcAc: 40 EtOH: 1 H₂O, the oxide concentration being fixed to 30 g/L. Sol-A was aged for 1 day before coating deposition.

A similar process was used to prepare titania sol-B but adding polyethylene PEG (average molecular weight of 400) to the ethanol-acidified water. Different PEG amounts (1, 3, 5 and 10 molar %), were incorporated maintaining the previous molar

ratios of precursors. Sol B was heated up to 80 °C for 1 hour to ensure the reactivity between titania oligomers and PEG [21].

Viscosity. The stability of the sols was studied through the evolution of viscosity with time, using a rheometer (Haake, RS50, Germany) under controlled rate conditions. The shear rate was increased from 0 to 1000 s⁻¹ in 5 min, with 1 min at the maximum rate and decreasing again to 0 in 5 min, at 25 °C.

2.2 Deposition and characterisation of coatings

Coatings deposition. A first layer of dense SiO₂ [37] (200 nm) was deposited onto the glass substrates to avoid the degradation of the photocatalytic activity [38]. This coating, with a 95 % of theoretical density, has demonstrated to inhibit the diffusion of Na⁺ cations from the glass substrate during firing [39,40].

TiO₂ films were deposited by dip-coating from TiO₂ sol-A and TiO₂ sol-B onto SiO₂ coated glass-slides and silicon wafers. The withdrawal rate varied from 5 to 60 cm/min. The coatings were treated in air at 350, 400, 450 and 500 °C for 1, 3 and 10 hours using heating and cooling rates of 10 °C/min. Finally, multilayer coatings of each sol were prepared using an intermediate treatment of 200 °C/ 30 min between depositions.

Optical and FE-SEM characterisation. Optical and Field-Emission Scanning Electron Microscopy (FE-SEM) (Hitachi-H7100, Japan) were used to study the homogeneity and microstructure of the coatings.

FTIR and GXRD characterisation. Coatings deposited onto silicon wafers were analysed by Fourier Transform Infrared Spectroscopy (FTIR) to study the structural evolution. FTIR spectra were recorded in transmission mode in the frequency range 4000 – 400 cm⁻¹ with a resolution of 2 cm⁻¹ using a Perkin Elmer FTIR (Spectrum 100 equipment). The crystallization of TiO₂ –anatase was followed by Grazing Angle X-Ray diffraction (GXRD) using Cu K_α radiation in a Bruker diffractometer (Siemens-D5000). The diffractogram was recorded in 2θ ranges of 20 – 70 ° and 23 – 27 °, using a fixed counting time of 20 s/step and 2θ increment of 0.03 °. The crystallite size (D) of the coatings sintered at 350, 400, 450 and 500 °C for 1, 3 and 10 hours was estimated using the Scherrer's equation:

$$D = \frac{0.9\lambda}{\beta \cos \theta_B} \quad [1]$$

where λ is the wavelength of K_α (0.15409 nm), β is the quartz standard-corrected full width at half-maximum (FWHM) of the Bragg Peak (rad) and θ_B is the Bragg angle ($^\circ$). The peak $2\theta_B = 25.2^\circ$ was chosen as the main peak for determining anatase phase. The crystal fraction evolution was followed through the area of this peak.

Specific surface area. The specific surface area was analysed as a function of temperature and time following a method described by A. Durán and M. Nieto [41]. Glass-microspheres with size between 40-70 μm were placed in a glass column closed by a filter. Sol-A and sol- B were dripped through the microspheres in the column and shaken in order to homogenize the system. Then, a flow of N_2 was passed through the column to dry the product. The coated microspheres were separated in four parts and heat treated at 350, 400, 450 and 500 $^\circ\text{C}$ for 1, 3 and 10 hours. The amount of TiO_2 deposited onto the microspheres was determined by chemical analysis (XRF, MagiX PW2424, Philip, Holland) and the surface area was measured by N_2 -adsorption BET method using a Monosorb Surface Area Analyser MS-13 (Quantachrome Co., USA). The surface area of the coatings was obtained through the equation:

$$\delta_{\text{TiO}_2} = \frac{\delta_{\text{measured}} - \delta_{\text{microspheres}}}{\text{TiO}_2 \text{ amount}} \quad [2]$$

where δ_{TiO_2} (m^2/g) is the surface are of TiO_2 coating; δ_{measured} (m^2/g) is the value obtained through BET method with the coated microspheres; $\delta_{\text{microspheres}}$ (m^2/g) is the surface area of the uncoated microspheres and TiO_2 amount, is the weight of TiO_2 obtained from chemical analysis.

Photocatalytic Activity. The photocatalytic properties of the supported photocatalysers were evaluated by studying the photocatalyst oxidation of trichloroethylene (TCE) as a model VOC's molecule in a continuous plug flow gas-phase flat photoreactor. This photoreactor, with external dimensions 120 x 50 x10 mm (length x wide x depth) was constructed in stainless steel except one window of 27 cm^2 , closed with borosilicate glass with low iron content. Illumination is provided by two UVA

Philips TL-8W/05 fluorescent lamps with a maximum emission at 365 nm wavelength and light intensity of 4.4 mW/cm². A gas mixture of TCE/ air was prepared using a gas cylinder of TCE/N₂ (Air Liquide, 500 ppm) and compressed air free of water and CO₂. The flow rate was controlled by using electronic mass flow controllers. The TCE concentration was maintained at 90 ppm, and the total gas flow was varied from 50 to 200 ml·min⁻¹ operating at residence time between 3.0 and 0.8 s. The TCE evolution with reaction time was analysed by gas chromatography using a Hewlett Packard HP6890 series with a Flame Injector Detector (FID).

3. RESULTS AND DISCUSSION

TiO₂ sols and films

Homogeneous and transparent sols were obtained for both compositions. Viscosity of TiO₂ sol-A and B with 1, 3, 5 and 10 molar % of PEG was measured at 25 °C. In all the cases, a Newtonian behaviour was observed with viscosities between 1.7 and 2 mPa.s. revealing a good stability during more than one month.

TiO₂ films were deposited by dip-coating from sol-A and sol-B using different withdrawal rates and heat treated at different temperatures and times. The coatings obtained from sol-A present good optical quality being homogeneous, transparent and crack free, with a critical thickness of 80 nm after treated at 500 °C/1h. In the case of sol-B, the coatings obtained with 5 and 10 molar % of PEG presented some defects and roughness, making difficult the thickness measurement. A molar ratio of 3 % was thus selected as the maximum amount of PEG compatible with homogeneous coatings. Under this condition, critical thickness of coatings with 3 % molar of PEG was found near of 100 nm after treatment at 500 °C/1h. This indicates that the addition of the surfactant generates thicker coatings compared to dense film, a phenomenon recently explained in porous coatings as the result of stress relaxation in pores [42].

Effect of sintering temperature and time in the crystallisation of TiO₂-anatase

The coatings prepared on silicon wafers from both sols were analysed by FTIR and GXRD to follow the crystallisation of TiO₂-anatase. FTIR spectra confirm that the coatings are free of organic residues. **Figure 1** shows the FTIR spectra of a) TiO₂-sol-A and b) TiO₂-sol-B coatings treated at 350 °C for different times. The band at 435 cm⁻¹ assigned to TiO₂ in anatase phase [43] is clearly observed. For coatings obtained from

sol- A the band is only detected for the longest treatment of 10 hours at 350 °C. However, coatings from sol-B show this band after only 3 h of thermal treatment at the same temperature, showing that the incorporation of PEG permits to reduce the sintering time. For higher temperatures, anatase band appears clearly after 1h of treatment. Thus, FTIR appears as a suitable and rapid method with high sensitivity to detect small amounts of anatase, though it is not strictly quantitative.

GXRD was further used to quantify the crystal size and area of peak (25.3°) as a function of temperature and sintering time. The area was calculated to evaluate the development of crystal fraction which is proportional to the area of the peak. The diffraction patterns of coatings of TiO₂ sol A and sol-B with 3% PEG treated at different temperatures and times were obtained in the 2θ range of 20-70° (not shown). The main band at 2θ ~ 25.3°, associated to the (101) lattice plane of the tetragonal TiO₂-anatase phase (JCPDS-89-4921) was identified in both types of coatings. A narrower interval of 2θ (23-27°) was further used to follow the evolution of the width and area of the anatase peak as a function of temperature and time of heat treatment. **Figure 2** shows the GXRD spectra in this range for coatings from sol B treated at 500 °C for 1, 3 and 10 h. The peak corresponding to anatase increases slowly and becomes narrower and more symmetric with the sintering time, indicating a better crystallisation and/or higher crystal fraction. Even using severe heat treatment conditions i.e. 500 °C/10 hours TiO₂- rutile phase was not observed.

Figure 3 shows the evolution of crystalline fraction, considered proportional to the area of (101) peak obtained from GXRD, as a function of temperature and time of the heat treatment. An important increment is observed for short treatments, associated with the rapid formation and/or growing of anatase crystals. Above 3 hours of heat treatment, the crystalline fraction maintains quite constant for T_≥400 °C. Coatings treated at 350 °C need a longer time (10 h) for total crystallisation.

The evolution of anatase crystal size (D) was estimated using the Scherrer's equation. The FWHM values were extracted from the XRD patterns fitted using the Peakfit software. The thickness and the calculated particle size of the coatings are represented in **Figure 4a)** and **4b)** as a function of temperature and sintering time. The coating thickness decreases with temperature and time of the thermal treatment due to contraction of the network associated with the sintering process. On the other hand, and

in spite of the error is quite high (around 5 %), an increasing trend in crystallite size with sintering temperature and time is apparent for 450 °C and 500 °C. At 400 °C the growing is much slower not being appreciable in the used time range. This behaviour is probably related with the activation energy necessary for an atom to leave the matrix and attach to the crystal that strongly depends on temperature [44]. A similar effect was observed in dense coatings obtained from sol-A.

Textural and morphological properties of TiO₂ thin films

Other relevant property related with photocatalytic activity is the specific surface area (S_s). Since no experimental techniques are available to measure this property in coatings an alternative procedure was used. Glass micro-spheres were coated with TiO₂ sols A and B with 3% of PEG and sintered at different temperatures and times. The specific surface area was measured by N₂ adsorption BET method and S_s of the coatings were calculated using the equation 2. **Figure 5** shows the specific surface area of the TiO₂ coatings sintered for 3 hours at different temperatures. At 350 °C low values of S_s are observed probably due to the incomplete removal of organic residues, still present in the structure. Above this temperature, S_s increases up to a maximum situated around 400-450 °C. For sol A this maximum (25 m²/g) maintains quite constant when temperature increases, indicating that maximum density has been reached around 400 °C. On the other hand, for TiO₂ sol-B, the maximum specific surface area is near 43 m²/g, suggesting coatings with more porous structure. When temperature increases S_s decreases and a gradual closing and collapse of the structure takes places, down to reach the S_s value of dense coatings from TiO₂-sol A. For these conditions (500 °C, 3h), similar results for both preparation routes were obtained.

The evolution of S_s with sintering time (1, 3 and 10 hours) was also studied observing a decrease likely associated with the partial collapse or densification of the coating structure.

Field Emission Scan Electron Microscopy (FE-SEM) was used to analyse the morphology (homogeneity and porosity) of the coated microspheres (**Figure 6**). Micrograph 6a) shows the total crystallisation of TiO₂ coating, with a narrow crystal size distribution centred around 27 nm, in good agreement with the values obtained by GXRD. Coatings produced by TiO₂-sol-B show a more porous structure compared with TiO₂-sol A, micrographs c) and b), confirmed by S_s measurements.

Photocatalytic activity

The effect of sintering time in the photocatalytic activity was evaluated for TiO₂ thin films prepared using sol-A and sol-B routes treated at 500 °C. The TCE conversion curves for TiO₂ samples prepared with a 3% PEG treated during 1, 3 and 10 hours are shown in Figure 7. Photocatalytic curves present similar trends, decreasing the TCE conversion with the sintering time and gas flow. A 90 % TCE conversion was obtained for 1 hour sintering time and 50 mL/min gas flow. When catalysts prepared from sol-A route were analysed similar results were obtained. As described in Figure 5, the specific surface area of coatings prepared from both sols and treated at 500 °C /3 h was similar and thus, a comparable photoactivity is expected. Longer sintering times lead to a decrease in the photocatalytic activity independent of the sol type. This effect is especially relevant when sintering time increases from 3 h to 10 h. According to previous data, TiO₂-anatase was the only phase detected, and crystal fraction and particle size do not significantly change with sintering time from 3 to 10 h. Thus, the reduction of photoactivity with sintering time should mainly be related to the densification of the coatings and the subsequent decrease of the surface area and porosity. Photoactivity data were collected in steady state conditions and deactivation of the catalyst was not observed.

The effect of the incorporation of PEG on the photocatalytic activity was also evaluated by comparing samples prepared from TiO₂-sol A and TiO₂-sol B treated at 450 °C during 3 hours through the degradation of TCE. The results are shown in Figure 8 varying the total gas flow from 50 ml·min⁻¹ to 200 mL/min. The results clearly show that the increase of porosity produced by the inclusion of PEG causes an augment of around 20% in the TCE conversion. The addition of PEG and its further elimination during the heat treatment lead to an increase of surface area and porosity of the samples reducing the internal mass transfer limitation of the pollutant to the active sites [45].

To make more visible this behaviour, we studied the influence of sintering temperature on the photoactivity of samples with 3% of PEG heat treated between 350 °C and 500 °C for 3 hours (coating thickness around 180 nm). **Figure 9** shows the TCE conversion values as a function of the treatment temperature for three different gas flows. A maximum is observed at 450 °C, corresponding to a TCE conversion higher than 90 %

at 50 mL/min. Higher treatment temperatures reduce the photoactivity of the coatings. X. Deng et al. obtained similar results for the gas-phase photo-oxidation of hexane over nano-size TiO₂ catalysts [46]. Zhu et al. [47] also analysed the effect of calcination temperatures (300-600 °C) in the degradation of phenol. According to DRIFT, XPS and XRD results, the authors conclude that heat treatments between 300-600 °C improve the degradation of phenol, as a consequent of a progressive elimination of the surface organic residue along with further crystallization in the TiO₂-anatase phase.

From these results, mainly those of BET and XRD analysis indicate that the photoactivity of titania coatings is closely related with the specific surface area. Although the presence of anatase is necessary, the crystal fraction and crystal size seem not to play a critical role in photocatalyst behaviour. These conditions implicate a compromise in temperature and times of sintering to ensure the appearance of TiO₂-anatase crystal phase, maintaining the high porosity of the layer.

4. CONCLUSIONS

Transparent, homogeneous and crack-free TiO₂-anatase nanocrystalline films were obtained through a simple and easy to scale-up sol-gel route incorporating PEG as pore generating agent.

The incorporation of PEG reduces the time necessary to obtain TiO₂- anatase to 3h/350 °C. GDXR showed that crystal size augments with temperature and time of heat-treatment with typical crystal size below 30 nm. The crystalline fraction increases sharply with sintering time, indicating that crystallisation is complete after 3 h.

High porosity and surface area implicate higher contact surface exposed to TCE thus enhancing the degradation rate. The highest TCE conversion was obtained with samples sintered at 450 °C/1 hour, the same conditions for obtaining the best compromise between the surface area and crystallinity. Further increase of sintering temperature causes a jumping down of the photocatalytic properties due to reduction of thickness and surface area related to densification of the coatings.

These results indicate that the photoactivity of titania coatings is closely related with the specific surface area. Although the presence of anatase is necessary, the crystal fraction and crystal size seem not to play a critical role in photocatalyst behaviour.

References

- [1] <http://www.epa.gov/iaq/voc.html>
- [2] EPA Act 1992 (Control of VOC Emissions from Petrol Storage & Distribution) Regulations (SI 374 of 1997)
- [3] Council Directive 2004/42/CE OF THE EUROPEAN PARLIAMENT L of 21 April 2004 on the limitation of emissions of volatile organic compounds due to the use of organic solvents in certain paints and varnishes and vehicle refinishing products and amending Directive 1999/13/EC.
- [4] M. A. Fox, M. Dulay, Chem. Rev. 83 (1995) 341.
- [5] J.-M. Herrmann, Topics in Catalysis. 34 (2005) 49.
- [6] O. Carp, C.L. Huisman, A. Reller, Progress in Solid State Chemistry 32 (2004) 33.
- [7] A. L. Linsebigler, G. Lu, J. T. Yates, J. Chem. Rev. 95 (1995) 735.
- [8] R. Portela, B. Sánchez, J.M. Coronado, R. Candal, S. Suárez, Catal. Today 129(1-2) 223.
- [9] S. Suárez, J. M Coronado, R. Portela, J.C: Martín, M. Yates, P. Avila, B. Sánchez, Env. Sci. Tech. 2008 (in press).
- [10] G. Balasubramanian, D. D. Dionysiou, M. T. Suidan, V. Subramanian, I. Baudin, J.M. Laïné, J.Mater. Sci. 38(4) (2003) 823.
- [11] Y. Chen, D.D. Dionysiou Appl. Catal. B 80 (2008) 147.
- [12] Y. Chen, S. Lunsford, D.D. Dionysiou Thin Solid Films (2008) *in press*.
- [13] D. Mergel, D. Buschendorf, S. Eggert, R. Grammes, B. Samser, Thin Solid Films 371 (2000) 218.
- [14]. S. Yamanoto, T. Sumita, A. Miyashita, H. Naramoto, Thin Solid Film 401 (2001) 88.
- [15]. J. Lee, M. Kim, B. Kim, Water Res. 36 (2002) 1776.
- [16] M. A. Fox and M. T. Dulay, Chem. Rev. 93 (1993) 341.
- [17] K. Kato, A. Tsuzuki, H. Taoda, Y. Torii, T. Kato, Y. Butsugan, J. Mater. Sci. 29 (1994) 5911.
- [18] H. Imai, H. Hirashima, J. Am. Ceram. Soc. 82 (1999) 2301.
- [19] J. H. Schattka, D. G. Schukin, J. Jia, M. Antonietti, R. A. Caruso, Chem. Mater. 14 (2002) 5103.
- [20]. U. Cernigoj, U. L. Stangar, P. Trebse, U. O. Krasovec, S. Gross, Thin Solid Film 495 (2006) 327.

- [21] S. Bu, Z. Jin, X. Liu, T. Yin, Z. Cheng, *J. Mater. Sci.* 41 (2006) 2067.
- [22] H. Choi, E. Stathatos, d. D. Dionysios, *Appl. Catal. B.* 63 (2006) 60.
- [23]. J. Yu, X. Zhao, J. Du, W. Chen, *Journal of Sol-Gel Science and Technology* 17 (2000) 163.
- [24] Y. Kotani, T. Matoda, A. Marsuda, T. Kogure, M. Tatsumisago, T. Minami, *J. Mater. Chem.* 11 (2001) 2045.
- [25] J. H. Schattka, e. H. M. Wong, M. Antonietti, R. A. Caruso, *J. Mater. Chem.* 16 (2006) 1414.
- [26] Y. Chen, E. Stathatos, D. D. Dionysiou, *Surf. Coat. Tech.* 202 (2008) 1994.
- [27] S. Bu, Z. Jin, X. Liu, H. Du, Z. Cheng, *J. Sol-gel Tench.* 30 (2004) 239.
- [28] K. Kajihara, T. Yao, *J. Sol-Gel Sci. Techn.* 17 (2000) 173.
- [29] K. Kajihara, K. Nakanishi, K. Tanaka, K. K. Hirao, N. Soga, *J. Am. Ceram. Soc.* 81 (1998) 2670.
- [30] K. Kajihara, T. Yao, *J. Sol-Gel Sci. Techn.* 12 (1998) 193.
- [31] A. Testino, I. R. Bellobono, V. Buscaglia, C. Canevali, M. D'Arienzo, S. Polizzi, R. Scotti, F. Morazzoni, *J. Am. Chem. Soc.* 129 (2007) 8566
- [32] H. Cheng, J. Ma, Z. Zhao, L. Qi, *Chem. Mater.* 7 (1995) 663.
- [33] Bacsa, R. R.; Kiwi, J. *Appl. Catal. B* 16 (1998) 19.
- [34] T. Peng, D. Zhao, K. Dai, W. Shi, K. Hirao, *J. Phys. Chem. B* 109 (2005) 4947.
- [35] D. Gumy, C. Morais, P. Bowen, C. Pulgarin, S. Giraldo, R. Hajdu, *J. Appl. Catal. B* 63 (2006) 76.
- [36] Yin, H.; Wada, Y.; Kitamura, T.; Kambe, S.; Murasawa, S.; Mori, H.; Sakata, T.; Yanagida, S. *J. Mater. Chem.* 11 (2001) 1694.
- [37] M. Guglielmi, S. Zenezini, *J. Non-Cryst. Solids* 121 (1990) 303.
- [38] J. Yu, X. Zhao, *Mater. Res. Bull.* 35 (2000) 1293.
- [39] G. S. Herman, Y. Gao, T. T. Tran, *Surf. Sci.* 447 (2000) 201.
- [40] M. Guglielmi, G. Brusatin, N. Tombolan, *Riv. Staz. Sper. Vetro Sup.* 23 (1993) 495.
- [41] A. Durán, M. I. Nieto, *Proceedings of XV Intern. Congress on Glass 2a* (1989) 5.
- [42] J. Gallardo, P. Galliano, A. Durán. *J. Sol-gel Sci. Techn.* 19 (2000) 393.
- [43] Y. Djaoued, S. Badilescu, P. V. Ashrit. D. Bersani, P. P. Lottici, *J. Sol-Gel Sci. Techn.* 24 (2002) 247.
- [44] Y. Li, T.J. White, S.H. Lim *J. Solid State Chemistry* 177 (2004) 1372.

- [45] S. Suárez, M. Yates, P. Avila, J. Blanco *Catal. Today* 105 (2005) 499.
- [46] X. Deng, Y. Yue, Z. Gao, *Appl. Catal. B* 39 (2002) 135.
- [47] J. Zhu, J. Yang, Z-F Bian, J. Ren, Y.-M. Liu, Y. Cao, H-X Li, H-Y He, K-N. Fan, *Appl. Catal. B* 76 (2007) 82.

FIGURE 1

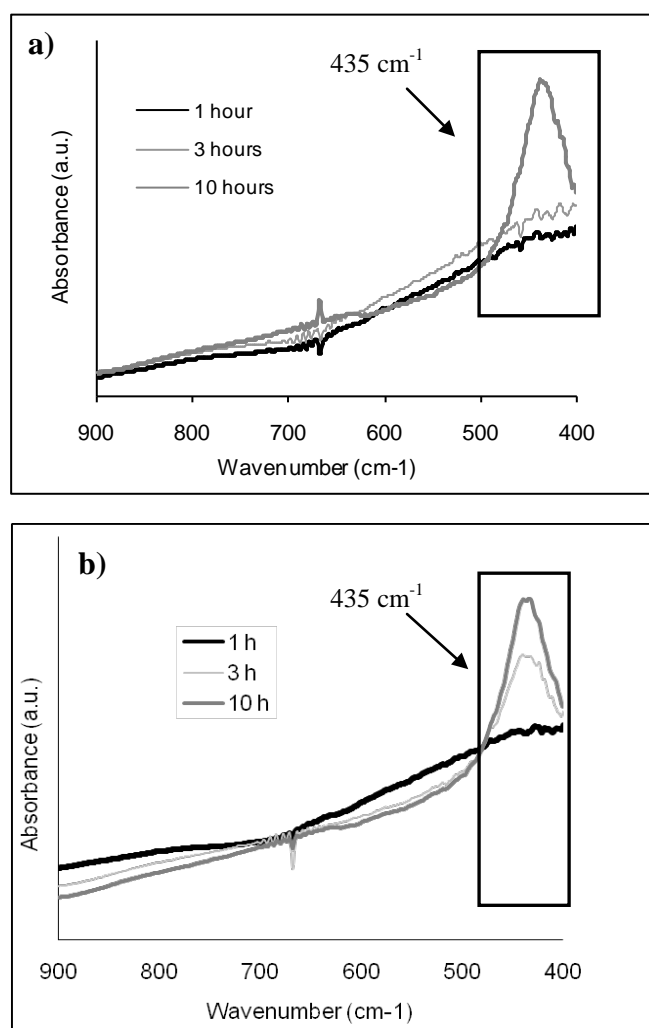


Figure 1. FTIR spectra of a) TiO₂ sol-A and b) TiO₂-sol-B treated at 350 °C for different times

FIGURE 2

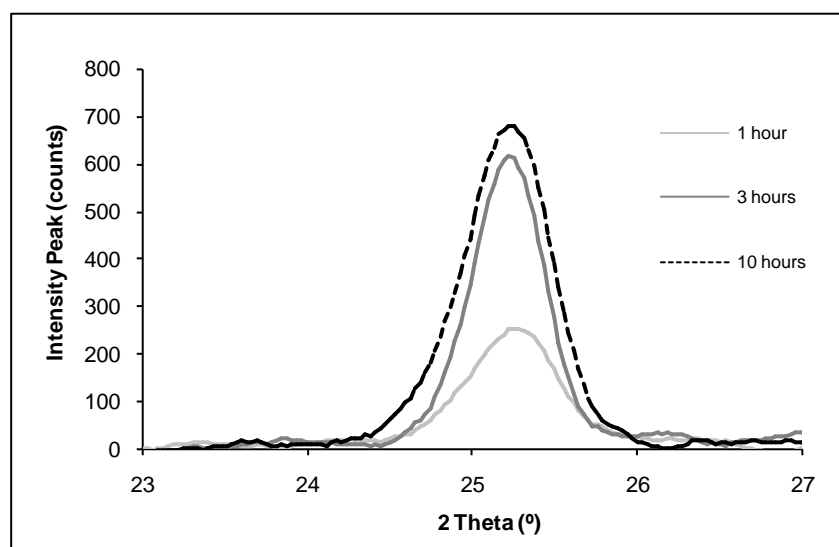


Figure 2. GXR D spectra of coatings from TiO_2 sol B treated at $500\text{ }^\circ\text{C}$ for different times

FIGURE 3

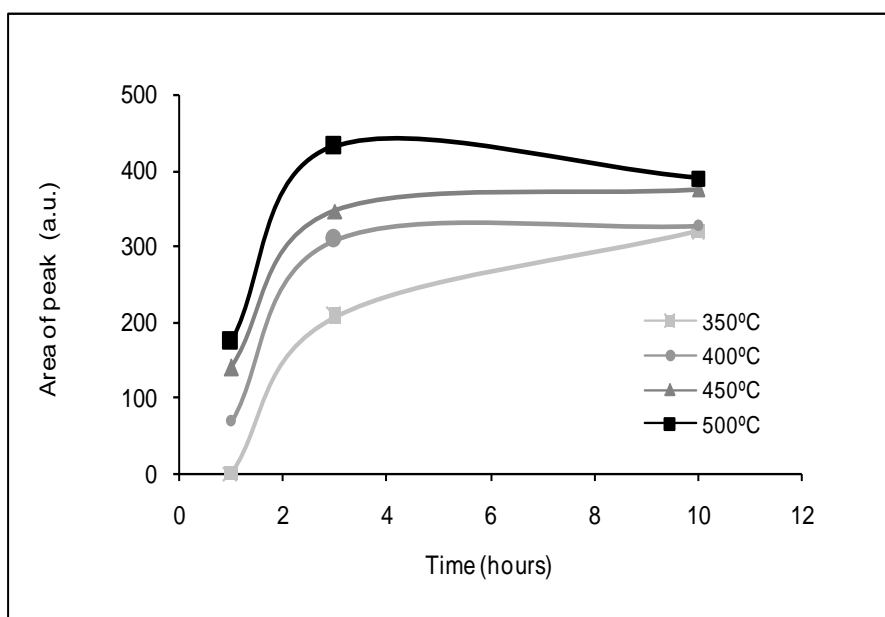


Figure 3. Area of GXR peaks (25.3°) on coatings from TiO_2 sol B for different heat treatments

FIGURE 4

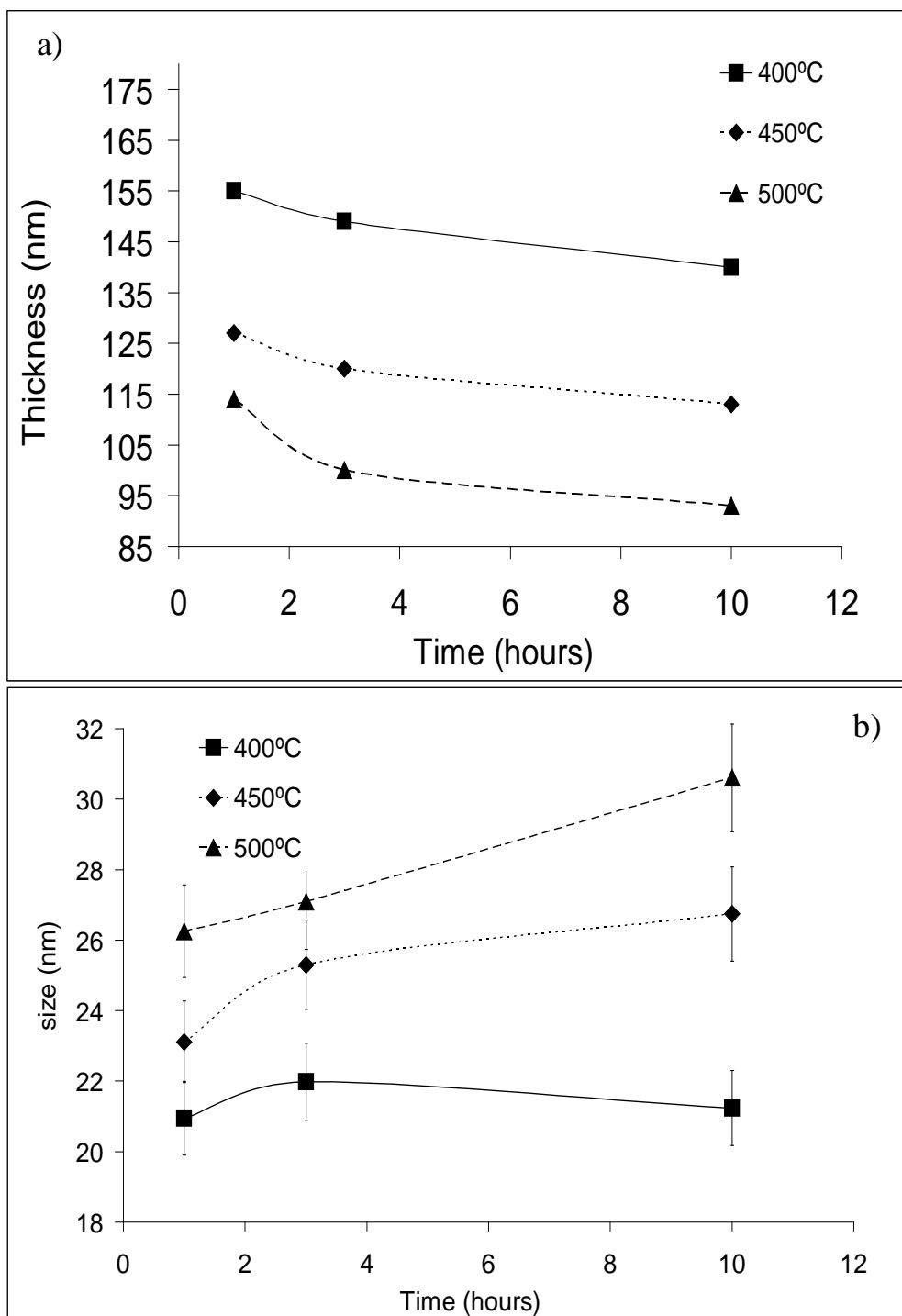


Figure 4. Thickness a) and crystal size b) of coatings obtained from TiO_2 sol B for different treatments

FIGURE 5

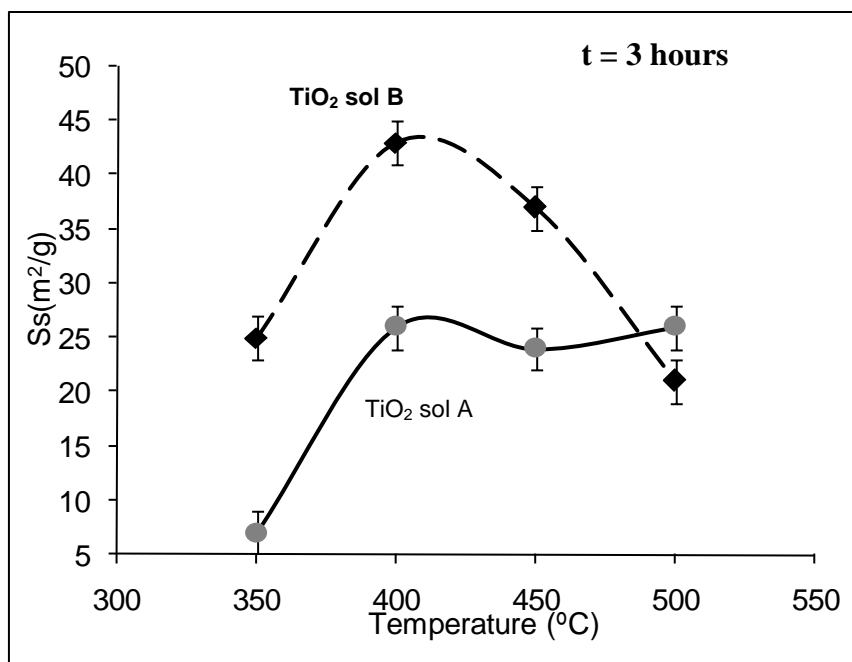


Figure 5. Specific surface area (S_s) of TiO_2 coatings from sol A and B as a function of sintering temperature

FIGURE 6

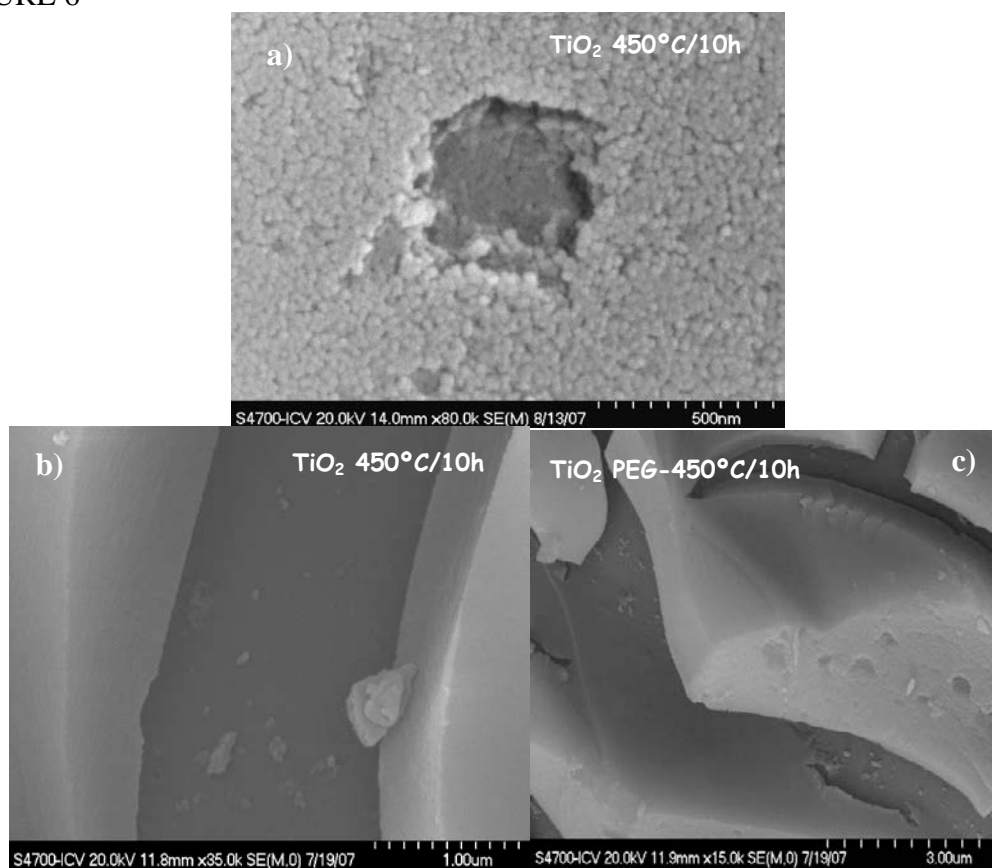


Figure 6. FE- SEM microphotographs of microspheres coated and treated at 450 °C for 10 hours from a) and b) TiO₂ sol A and c) TiO₂ sol B

FIGURE 7

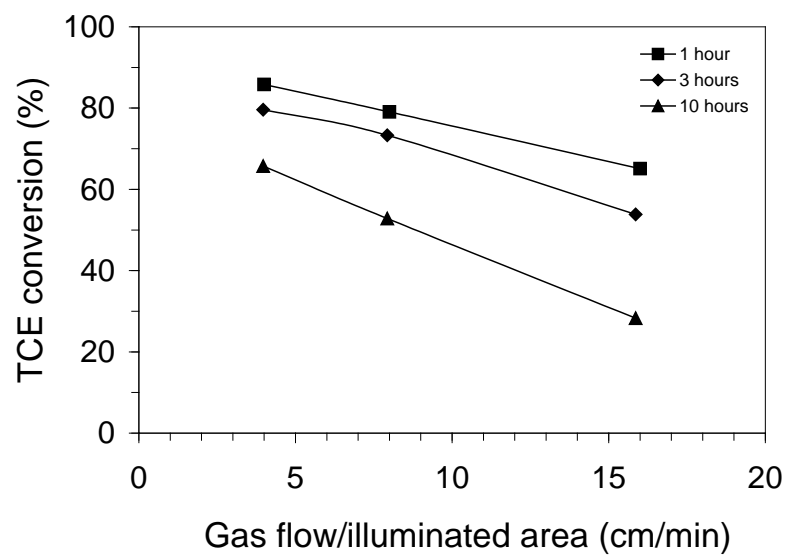


Figure 7. Effect of the sintering time in the TCE conversion as a function of the total gas flow referred to illuminated area for samples prepared from TiO_2 sol B treated at 500 °C

FIGURE 8

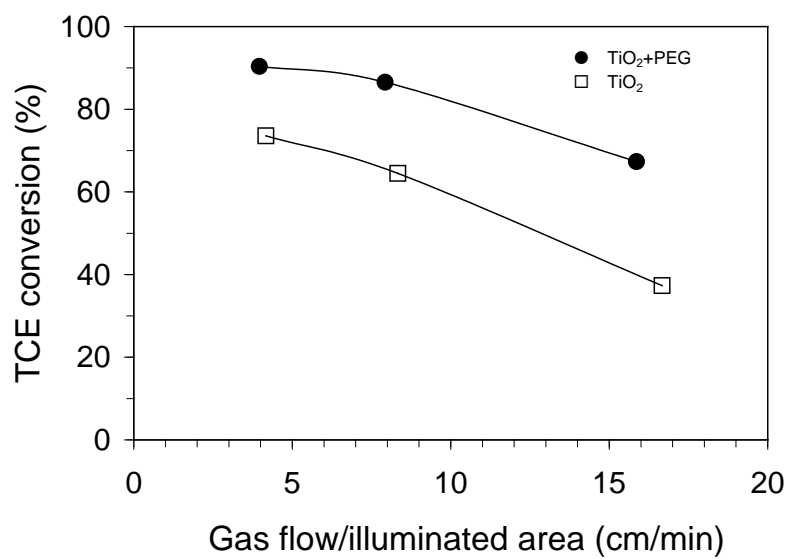


Figure 8. Influence of the incorporation of PEG in the photocatalytic activity for samples treated at 450 °C during 3 hours

FIGURE 9

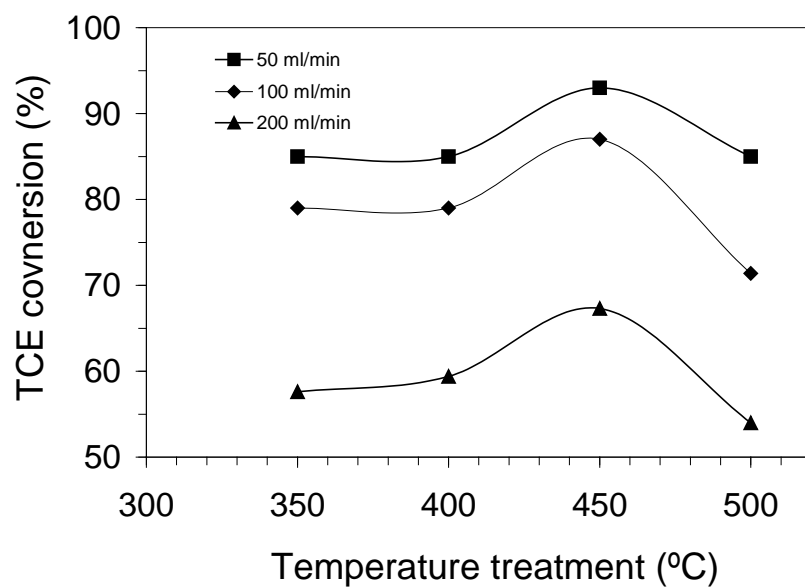


Figure 9. Influence of the sintering temperature in the photocatalytic activity for two-layer coatings prepared by sol B with a 3% PEG for different total gas flow